SCIENCE CHINA
Information Sciences

• **Supplementary File** •

A variable threshold visual sensing and image reconstruction method based on pulse sequence

Jiangtao XU[1,2], Peng LIN[1,2], Zhiyuan GAO[1,2*], Kaiming NIE[1,2] & Liang XU[1,2]

[1]*School of Microelectronics, Tianjin University, Tianjin* 300072*, China;*
[2]*Tianjin Key Laboratory of Imaging and Sensing Microelectronic Technology, Tianjin* 300072*, China*

Appendix A Operation principle and error analysis of pulse-based sensing mechanism

The architecture of pulse-based image sensor is shown in Figure A1(a). The sensor is composed of pixel array, row selector, column digital buffer, threshold generator, ramp generator and logic control circuit. Threshold generator provides trigger threshold for pixel array. Ramp generator enables the threshold to vary with time. Each time the row selector picks a row, signals in the row are transmitted through parallel buses to the column digital buffer. Pixels are read out row by row, whether triggered or not. The scan time of entire pixel array is defined as frame period. Column digital buffer is used to receive pulse data and the buffer will convert the parallel data to the serial output.

The structure of the spiking pixel is given in the letter. The working process of the pixel is shown in A1(b). It includes photo-measurement stage and reset stage. In reset stage, a pulse is applied to the reset transistor, resetting the photodiode to a predefined voltage level V_{rst}. In photo-measurement stage, photocurrent discharges the photodiode. When PD's voltage reaches the threshold voltage V_{th}, the comparator output a pulse. The time from the start of integration to the comparator triggered is defined as integration time. When the row selection signal arrives, the photodiode is reset and the trigger state is readout through the column bus. The process from the start of integration to the readout of the triggered pulse is defined as a trigger cycle.

$T_{\mathrm{p},i}$ represents the integration time of i-th trigger cycle. The relationship between $T_{\mathrm{p},i}$ and I_{ph} is:

$$C_{\mathrm{PD}} \cdot (V_{\mathrm{rst}} - V_{\mathrm{th}}) = \int_{t_0}^{t_0+T_{\mathrm{p},i}} I_{\mathrm{ph}}(t)\,\mathrm{d}t, \tag{A1}$$

where t_0 is the time point when the integration starts.

In i-th trigger cycle, the average received photocurrent is restored by:

$$I_{\mathrm{ph}} = \frac{C_{\mathrm{PD}} \cdot (V_{\mathrm{rst}} - V_{\mathrm{th}})}{T_{\mathrm{p},i}}. \tag{A2}$$

When the row selection signal arrives, if the pixel has been triggered in the frame cycle, pixel outputs '1', which indicates a pulse. Otherwise, pixel outputs '0'. The trigger interval of the i-th trigger cycle, N_i, is obtained by the amount of '0's between two adjacent pulses. The integration time $T_{\mathrm{p},i}$ can be estimated from N_i according to:

$$T_{\mathrm{p},i} = N_i \cdot T_{\mathrm{u}} - T_{\mathrm{wait}}, 0 < T_{\mathrm{wait}} \leqslant T_{\mathrm{u}}, \tag{A3}$$

where T_{u} is frame period, T_{wait} is the waiting time from the comparator triggered to the pulse readout. The waiting time varies with photocurrent. Due to the uncertainty of waiting time, the actual time point of pulse generated cannot be acquired from the outputs.

As parameter C_{PD}, V_{rst} and V_{th} are considered constant in the pixel array, the relative error of the restored photocurrent introduced by T_{wait} is:

$$\Delta I_{\mathrm{ph}}/I_{\mathrm{ph}} = T_{\mathrm{wait}}/T_{\mathrm{p},i}, \tag{A4}$$

where ΔI_{ph} is the deviation of the restored photocurrent from the actual received photocurrent. The relative error of the restored photocurrent is proportional to T_{wait}. For different received photocurrent mapped to the same trigger interval, it is assumed that T_{wait} follows the uniform random distribution of 0 to T_{u}. The standard deviation of the relative error is given by:

* Corresponding author (email: gaozhiyuan@tju.edu.cn)

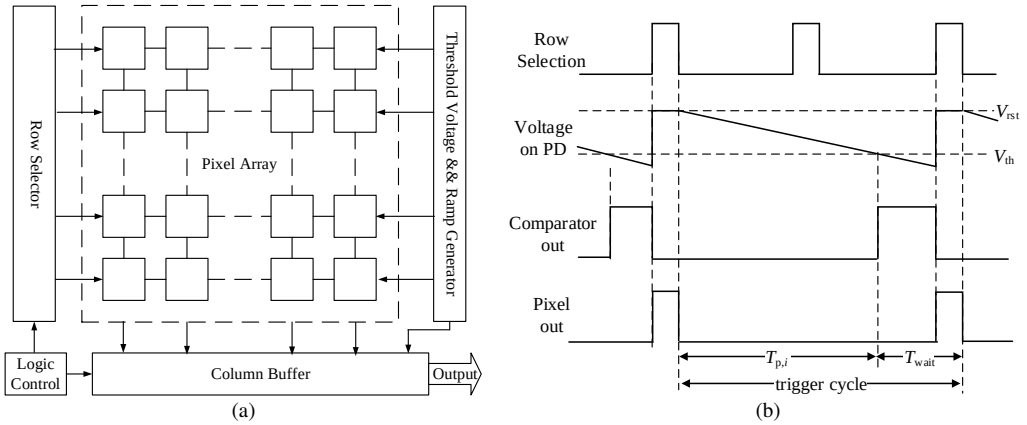

Figure A1 (a) The structure of the pulse-based image sensor; (b) The working process of the pixel.

$$\sigma\left(\frac{\Delta I_{\rm ph}}{I_{\rm ph}}\right)=\frac{1}{2\sqrt{3}}\frac{I_{\rm ph}\cdot T_{\rm u}}{C_{\rm ph}\cdot(V_{\rm rst}-V_{\rm th})}. \tag{A5}$$

The relative error of the restored photocurrent induced by the waiting time can be considered as readout noise. The standard deviation of this noise increases proportionally with photocurrent. Under high illumination conditions, the noise can cause severe degradation of image quality. It is possible to suppress the noise by increasing the integration voltage range, $V_{\rm rst}-V_{\rm th}$, in (A5). However, this method has a negative impact on pixels' response speed. According to (A2), the integration time is proportional to $V_{\rm rst}-V_{\rm th}$ under the same light condition. The pixel's response will slow down when $V_{\rm rst}-V_{\rm th}$ rises. It limits the sensor's performance, especially in low illumination environments.

In image reconstruction, the gray value Y can be calculated by:

$$Y=\left[\frac{I_{\rm ph}}{I_{\rm pmax}}\left(2^{N_{\rm id}}-1\right)\right]=\left[\frac{N_{\rm max}}{N_i}\left(2^{N_{\rm id}}-1\right)\right], \tag{A6}$$

$I_{\rm pmax}$ is the input photocurrent maped to the largest gray value and is called maximum mapping photocurrent. $N_{\rm max}$ is the equivalent trigger interval at $I_{\rm pmax}$. In the reconstruction, it is required that every gray value can be mapped by a trigger interval. The trigger interval which is mapped to the second largest gray value $2^{N_{\rm id}}-2$, is expressed as $N_{\rm max}+D$. In the sensing scheme with fixed threshold, D is an integer and its minimum value is 1. According to (A2) and (A6), the maximum mapping photocurrent can be expressed as:

$$I_{\rm pmax}=\frac{V_{\rm rst}-V_{\rm th}}{D\cdot T_{\rm u}}C_{\rm PD}\left(\frac{1}{2^{N_{\rm id}}-2}\right). \tag{A7}$$

Limited by frame period, the maximum photocurrent $I_{\rm pp}$ that can be perceived by the sensor is:

$$I_{\rm pp}=\frac{V_{\rm rst}-V_{\rm th}}{T_{\rm u}}C_{\rm PD}. \tag{A8}$$

In normal grayscale images, image depth is 8, and the maximum mapping photocurrent is required to be at least 253 times lower than $I_{\rm pp}$. Otherwise, the number of gray levels in reconstructed images will be reduced. In the case of $N_{\rm max}$ set to 1, two smallest trigger intervals, 1 and 2, are mapped to gray values 255 and 128 according to (A6), respectively. The gray levels between 255 and 128 are lost in the reconstructed image, resulting in information loss and deterioration of image quality. On account of readout noise and information loss, it is hard to capture very high illumination scene based on fixed threshold voltage, resulting in limited dynamic range.

In the proposed variable threshold sensing scheme, the difference between equivalent trigger intervals can be much smaller than 1. The parameter, D, in (A7) is decreased and the limit of maximum mapping photocurrent is relieved. Under the same maximum mapping photocurrent, the gray scale distribution can be improved, and the richer information can be reconstructed.

In pixels working based on fixed threshold, the integration time is in the range of $(N_i-1)\,T_{\rm u}$ to $N_iT_{\rm u}$ according to (A3). The trigger interval N_i in different trigger cycles is constant as long as the photocurrent does not change. No matter how many trigger cycles are taken into account, the restored photocurrent and the reconstructed image cannot get higher accuracy. The variable threshold allows the trigger interval to change in different trigger cycles, and so the range of restored photocurrent is able to change with trigger cycle. The equivalent trigger interval of the trigger window is limited in the range of $N_{{\rm equ},g}$ to $N_{{\rm equ},m}$. As window depth increases, the calculated $N_{{\rm equ},m}$ and $N_{{\rm equ},g}$ will get closer. The equivalent trigger interval can be restored more accurately and the restored photocurrent $I_{\rm cal}$ will be closer to the actual photocurrent, leading to lower readout noise.

Appendix B Proof of Proposition 1-3

Appendix B.1 Proof of Proposition 1

In the i-th trigger cycle, PD's integrated voltage V_{int} is a function of time t, which can be expressed as:

$$V_{\text{int}}(t) = V_{\text{rst}} - \frac{I_{\text{ph}} \cdot t}{C_{\text{PD}}}. \tag{B1}$$

According to the definition of N_i, the pixel is triggered in the N_i-th frame cycle. Therefore, at the end of the N_i-th frame cycle, the relationship between the integrated voltage and the threshold is given by:

$$V_{\text{int}}(N_i \cdot T_{\text{u}}) > V_{\text{th},i}. \tag{B2}$$

In the $(N_i - 1)$-th frame cycle, the pixel does not triggered and the threshold is $V_{\text{th},i} - V_{\text{s}}$. At the end of the $(N_i - 1)$-th frame cycle, the relationship between the threshold and the integrated voltage is given by:

$$V_{\text{int}}((N_i - 1) \cdot T_{\text{u}}) \leqslant V_{\text{th},i} - V_{\text{s}}. \tag{B3}$$

Substituting (B1) into (B2) and (B3) can directly yield Proposition 1.

Appendix B.2 Proof of Proposition 2

In a trigger window, the restored photocurrent is in the intersection set of different ranges calculated according to Proposition 1. Therefore, the lower limit of restored photocurrent is calculated by:

$$I_{\text{min}} = \max\left\{\frac{C_{\text{PD}} \cdot \left(V_{\text{rst}} - V_{\text{th},i}\right)}{N_i \cdot T_{\text{u}}}\right\}, i = 1, 2, \cdots, n, \tag{B4}$$

Similarily, the higher limit of restored photocurrent is calculated by:

$$I_{\text{max}} = \min\left\{\frac{C_{\text{PD}} \cdot \left(V_{\text{rst}} - V_{\text{th},i} + V_{\text{s}}\right)}{(N_i - 1) \cdot T_{\text{u}}}\right\}, i = 1, 2, \cdots, n, \tag{B5}$$

According to Definition 2, I_{min}, I_{max} and I_{cal} are given by:

$$I_{\text{min}} = \frac{C_{\text{PD}} \cdot (V_{\text{rst}} - V_{\text{th0}})}{N_{\text{equ},m} \cdot T_{\text{u}}}, \tag{B6}$$

$$I_{\text{max}} = \frac{C_{\text{PD}} \cdot (V_{\text{rst}} - V_{\text{th0}})}{N_{\text{equ},g} \cdot T_{\text{u}}}, \tag{B7}$$

$$I_{\text{cal}} = \frac{C_{\text{PD}} \cdot (V_{\text{rst}} - V_{\text{th0}})}{N_{\text{equ}} \cdot T_{\text{u}}}, \tag{B8}$$

respectively. Combining (B4) and (B6) yields:

$$N_{\text{equ},m} = \min\left\{\frac{N_i}{1 - a \cdot Nf_i}\right\}, i = 1, 2, \cdots, n, \tag{B9}$$

$$a = V_{\text{s}} / \left(V_{\text{rst}} - V_{\text{th0}}\right), \tag{B10}$$

$$Nf_i = \left(V_{\text{th},i} - V_{\text{th0}}\right) / V_{\text{s}}. \tag{B11}$$

where a is a system parameter, Nf_i is the interval between the pixel pulse output in the i-th trigger cycle and the immediately prior ramp pulse.

Combining (B5) and (B7) yields:

$$N_{\text{equ},g} = \max\left\{\frac{N_i - 1}{1 - a \cdot (Nf_i - 1)}\right\}, i = 1, 2, \cdots, n, \tag{B12}$$

The restored photocurrent I_{cal} is the average of I_{min} and I_{max} and is given by:

$$I_{\text{cal}} = \frac{I_{\text{max}} + I_{\text{min}}}{2} = \frac{C_{\text{PD}} \cdot (V_{\text{rst}} - V_{\text{th0}})}{T_{\text{u}}} \cdot \frac{N_{\text{equ},g} + N_{\text{equ},m}}{2 N_{\text{equ},g} N_{\text{equ},m}} \tag{B13}$$

Combining (B8) and (B13) yields:

$$N_{\text{equ}} = \frac{2 N_{\text{equ},g} N_{\text{equ},m}}{N_{\text{equ},g} + N_{\text{equ},m}}. \tag{B14}$$

Appendix B.3 Proof of Proposition 3

If the photocurrent does not change during two consecutive trigger cycles, according to (A2), (B10) and (B11), we get the following equation:

$$\frac{T_{\mathrm{p},i+1}}{T_{\mathrm{p},i}} = \frac{V_{\mathrm{rst}} - V_{\mathrm{th},i+1}}{V_{\mathrm{rst}} - V_{\mathrm{th},i}} = \frac{1 - a \cdot Nf_{i+1}}{1 - a \cdot Nf_i}, \tag{B15}$$

The value of $T_{\mathrm{p},i}$ and $T_{\mathrm{p},i+1}$ can be estimated from the trigger intervals according to (A3). The photocurrent can be considered constant during the two trigger cycles if the relationship between $T_{\mathrm{p},i}$ and $T_{\mathrm{p},i+1}$ satisfies:

$$\frac{N_{i+1} - \zeta}{N_i} < \frac{T_{\mathrm{p},i+1}}{T_{\mathrm{p},i}} < \frac{N_{i+1}}{N_i - \zeta}, \tag{B16}$$

where ζ is the error tolerance which is set to adjust the probability that (B16) holds. The error tolerance is set in the range of 0 to 1 as the measurement error of trigger interval is in the range of 0 to 1. When ζ is small, due to the readout noise induced by waiting time, formula (B16) may not hold even the photocurrent is constant. As ζ increases, formula (B16) is more likely to hold even if the photocurrent has changed, and the change of photocurrent is more likely to be ignored.

According to (B15) and (B16), the illumination can be considered constant in the case of:

$$\frac{N_{i+1} - \zeta}{N_i} < \frac{1 - a \cdot Nf_{i+1}}{1 - a \cdot Nf_i} < \frac{N_{i+1}}{N_i - \zeta}, \tag{B17}$$

Appendix C Experiment results

To verify the effectiveness of the proposed reconstruction method, behavioral models of visual sensing based on fixed threshold and variable threshold are built, respectively. Both the models of the image sensor are with a size of 250 columns and 250 rows. The frame period of the sensor is 25 μs. The capacitance of the photodiode C_{PD} is 5 fF. The reset voltage V_{rst} is 3 V. The minimum threshold V_{th0} is 2 V and the maximum threshold $V_{\mathrm{th,max}}$ is 2.6 V. The fixed threshold voltage V_{th} is set equal to V_{th0}.

Appendix C.1 Noise suppression

A group of photocurrent which satisfies the uniform distribution from minimum value I_{pmin} to maximum mapping photocurrent I_{pmax} is used as the input of the sensor model. Measurement errors under different input current conditions are analyzed. The relative error RE and the average relative error RE_{ave} of the photocurrent are calculated by:

$$RE\left(I_{\mathrm{in}}\right) = \frac{\left|I_{\mathrm{in}} - I_{\mathrm{cal}}\left(I_{\mathrm{in}}\right)\right|}{I_{\mathrm{in}}}, \tag{C1}$$

$$RE_{\mathrm{ave}} = \frac{1}{I_{\mathrm{pmax}} - I_{\mathrm{pmin}}} \int_{I_{\mathrm{pmin}}}^{I_{\mathrm{pmax}}} RE\left(I_{\mathrm{in}}\right) \mathrm{d}I_{\mathrm{in}}, \tag{C2}$$

where I_{in} is the input photocurrent and I_{cal} is the restored photocurrent.

To cover the range of ambient light intensity where image sensor usually works, we set I_{pmin} to 0.1 pA and set I_{pmax} to 45 pA. The model converts input photocurrent to equivalent trigger interval N_{equ} in the way described in Proposition 2. And the restored photocurrent is calculated according to (B13). The relationship among average relative error, step height and window depth is shown in Figure C1. Step height is in the range of 0 mV to 6 mV. The mean relative error is 2.76% with $V_{\mathrm{s}} = 0$ mV, which corresponds to the case of pixel working based on fixed threshold. When the step height is relatively small, the average relative error decreases rapidly with the increase of step height. The average relative error reaches the minimum value when step height is about 3.5 mV. As the step height continues to increase, the average relative error slightly increases, but it is still much smaller than that with fixed threshold. The window depth n is in the range of 1 to 10. The average relative error decreases significantly as window depth increases. When the step height is 3.5 mV, the average relative error is reduced to 1.13% with window depth set to 5 and 0.53% with window depth set to 10. The result shows that readout noise can be suppressed significantly even with a small window depth.

The relationship between relative error and the photocurrent is shown in Figure C2. According to (A5), the standard deviation of the relative error is proportional to photocurrent. When the input photocurrent is small, all the curves show small relative error. As input photocurrent increases from I_{pmin} to I_{pmax}, the overall relative error with fixed threshold shows a significant upward trend. The relative error with variable threshold is not so sensitive to the change of input photocurrent and is significantly lower than that with fixed threshold in high light conditions. The larger the window depth is, the smaller the relative error is.

The shape of the relative error curve is like a triangular wave. Input photocurrent between two adjacent peaks of the curve is mapped to one equivalent trigger interval and will result in the same restored photocurrent which is given by (B13). The minimum input photocurrent mapped to the equivalent trigger interval is given by (B4), where the integration time is larger than $N_{\mathrm{equ}}T_{\mathrm{u}}$. As input photocurrent increases from the minimum value to the restored value, the integration time of the pixel gets closer to $N_{\mathrm{equ}}T_{\mathrm{u}}$ and the relative error deceases to zero. As input photocurrent continues to increase to the maximum value mapped to the same equivalent trigger interval, the integration time gets smaller than $N_{\mathrm{equ}}T_{\mathrm{u}}$, and the relative error increases. In fixed threshold sensing scheme, a large range of input photocurrent may be mapped to the same trigger interval, leading to a large maximum deviation of restored photocurrent from input photocurrent. Whereas in the

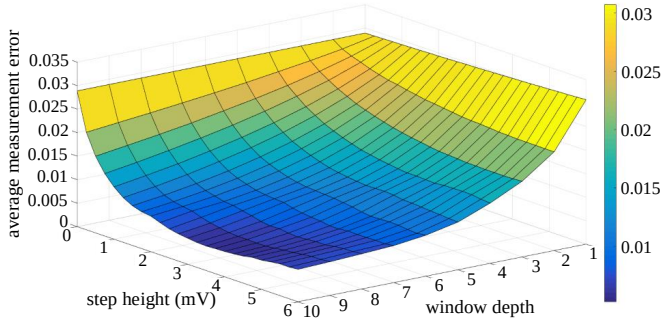

Figure C1 The relationship among average measurement error, step height and window depth.

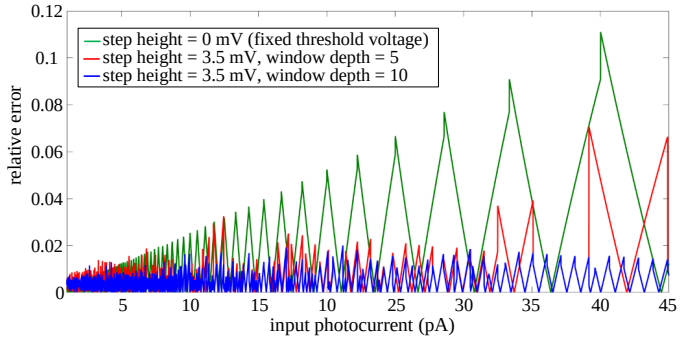

Figure C2 The relationship between relative error and input photocurrent.

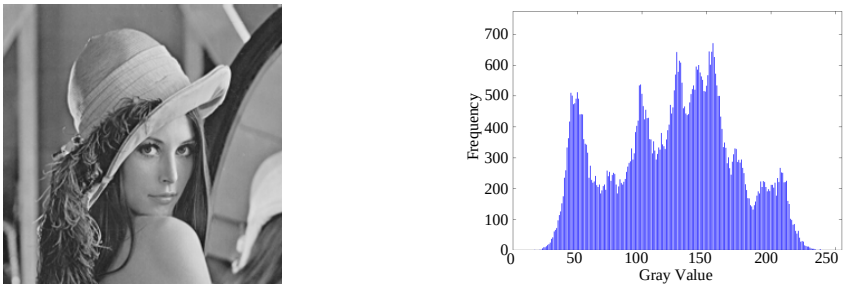

Figure C3 (a) Input image; (b) its gray scale distribution histogram.

variable threshold sensing scheme, the range of input photocurrent covered by the same trigger interval is much smaller, leading to smaller maximum deviation in photocurrent restoration. Therefore, the relative error and the average relative error are much smaller.

Appendix C.2 Image reconstruction for static scene

To explore the quality of reconstructed images, a static image is used as the input of the sensor model to generate pulse sequences. The pulses are reconstructed to a gray-scale image which is compared with the input image. In the reconstruction, the model converts the equivalent trigger interval to the corresponding gray value in the way described in the letter. Figure C3 shows the original image and its gray scale distribution histogram. Figure C4 shows the reconstructed images with different maximum mapping photocurrent and window depth. Figure C5 shows their gray scale distribution histograms.

To analyze the quality of the reconstructed image further, the mean square error (MSE) analysis is carried out. The MSE result is calculated by:

$$MSE = \frac{1}{M \times N} \sum_{k=1}^{M} \sum_{j=1}^{N} \left(Y_{\mathrm{r}}(k,j) - Y_{\mathrm{o}}(k,j) \right)^2, \tag{C3}$$

where M is the row number of the image, N is the column number of the image. Parameter $Y_{\mathrm{r}}(k,j)$ is the gray-scale value of the pixel at k-th row and j-th column in the reconstructed image. Parameter $Y_{\mathrm{o}}(k,j)$ is the gray-scale value of the pixel at k-th row and j-th column in the original image. The smaller the MSE is, the more similar the two images are.

(a) fixed $V_{\rm th}$, $I_{\rm pmax}$ = 10 pA (b) fixed $V_{\rm th}$, $I_{\rm pmax}$ = 30 pA (c) fixed $V_{\rm th}$, $I_{\rm pmax}$ = 45 pA

(d) $n = 5$, $I_{\rm pmax}$ = 10 pA (e) $n = 5$, $I_{\rm pmax}$ = 30 pA (f) $n = 5$, $I_{\rm pmax}$ = 45 pA

(g) $n = 10$, $I_{\rm pmax}$ = 10 pA (h) $n = 10$, $I_{\rm pmax}$ = 30 pA (i) $n = 10$, $I_{\rm pmax}$ = 45 pA

Figure C4 The reconstructed images. (a), (b), and (c) are images reconstructed based on fixed threshold, with maximum mapping current 10 pA, 30 pA, and 45 pA, respectively. (d), (e), and (f) are images reconstructed based on variable threshold and window depth 5, with maximum mapping current 10 pA, 30 pA, and 45 pA, respectively. (g), (h), and (i) are images reconstructed based on variable threshold and window depth 10, with maximum mapping current 10 pA, 30 pA, and 45 pA, respectively.

The MSE results of the reconstructed images are shown in Table C1. With maximum mapping photocurrent set to 10 pA, the reconstructed images are much more similar to the original image. As the trigger time is inversely proportional to the received photocurrent, a larger range of photocurrent will be mapped to one trigger cycle under high light conditions. In the fixed threshold sensing method, as the maximum mapping photocurrent grows up, more different gray levels in the original image are mapped to the same gray level in the reconstructed image as shown in Figure C5. Due to the loss of gray levels, the information of reconstructed images is reduced and the images seem to be overexposed. With photocurrent increases from 10 pA to 45 pA, the MSE increases from 1.5033 to 26.0006. In the sensing method based on variable threshold, the image quality is less sensitive to the change of maximum mapping photocurrent. As shown in Figure C4 and Figure C5, more gray levels can be restored and richer information can be reconstructed with the increase of window depth. When maximum mapping photocurrent increases from 10 pA to 45 pA, the MSE increases from 0.7277 to 2.8713 with window depth set to 5 and from 0.4041 to 1.0440 with window depth set to 10. The proposed image reconstruction method shows a better performance than traditional method, especially in high illuminated conditions.

To show the effect of this method more intuitively, an image whose background shows a grayscale gradient is used as the input of the model with $I_{\rm pmax}$ set to 30 pA and the results are shown in Figure C6 and Table C2. In reconstruction method based on fixed threshold, obvious stripes appear in the high illuminated place. In the image reconstructed based on variable threshold, the stripes fade away as the window depth increases.

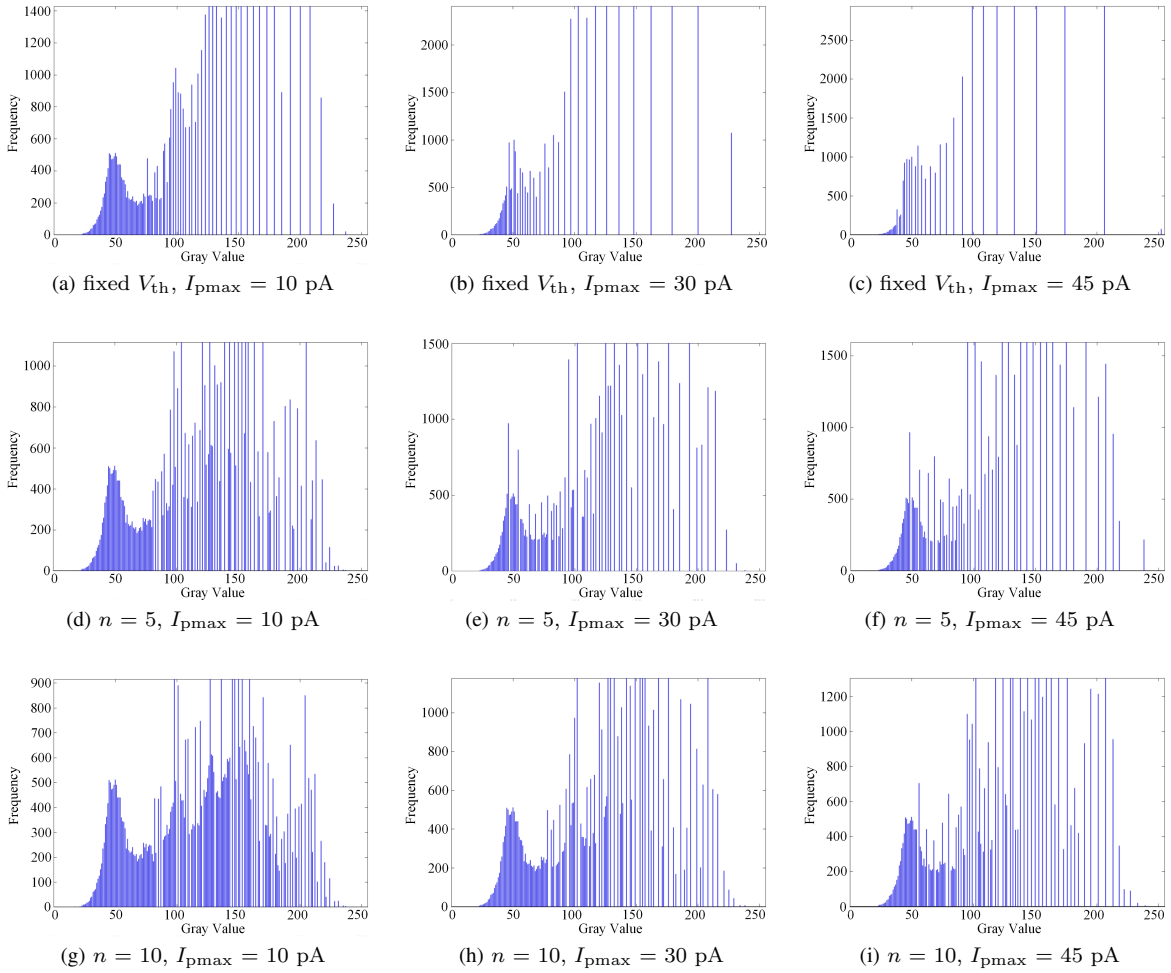

(a) fixed $V_{\rm th}$, $I_{\rm pmax}$ = 10 pA (b) fixed $V_{\rm th}$, $I_{\rm pmax}$ = 30 pA (c) fixed $V_{\rm th}$, $I_{\rm pmax}$ = 45 pA

(d) n = 5, $I_{\rm pmax}$ = 10 pA (e) n = 5, $I_{\rm pmax}$ = 30 pA (f) n = 5, $I_{\rm pmax}$ = 45 pA

(g) n = 10, $I_{\rm pmax}$ = 10 pA (h) n = 10, $I_{\rm pmax}$ = 30 pA (i) n = 10, $I_{\rm pmax}$ = 45 pA

Figure C5 Gray scale distribution histogram of the reconstructed images. (a), (b), and (c) are gray scale distribution of images reconstructed based on fixed threshold, with maximum mapping current 10 pA, 30 pA, and 45 pA, respectively. (d), (e), and (f) are gray scale distribution of images reconstructed based on variable threshold and window depth 5, with maximum mapping current 10 pA, 30 pA, and 45 pA, respectively. (g), (h), and (i) are gray scale distribution of images reconstructed based on variable threshold and window depth 10, with maximum mapping current 10 pA, 30 pA, and 45 pA, respectively.

Table C1 MSE result of reconstructed static images shown in Figure C4

$I_{\rm pmax}$(pA)	10	30	45
MSE with fixed threshold	1.5033	13.7957	26.0006
MSE with window depth =5	0.7277	1.7210	2.8713
MSE with window depth =10	0.4041	0.7773	1.0440

Table C2 MSE results of reconstruction static images shown in Figure C6

	Fixed threshold	Window depth = 5	Window depth = 10
MSE	8.7691	1.6146	0.7284

Appendix C.3 Image reconstruction for dynamic scene

To investigate the effect of the adaptive reconstruction method for dynamic scene, a high-speed sensing experiment is performed. A video with 10000 fps is used as the input of the model. In the reconstruction, the model adaptively selects the value of window depth according to Proposition 3 with ζ set to 0.5. The maximum mapping photocurrent $I_{\rm pmax}$ is set from 3 pA to 45 pA. The frames in original video and reconstructed videos with various light conditions are shown in Figure C7. Their MSE results are shown in Table C3.

MSE analysis is also performed on the reconstructed video and its result is given by:

(a) (b) (c) (d)

Figure C6 The original images and reconstructed images. (a) the original image; (b) image reconstructed based on fixed threshold; (c) image reconstructed based on variable threshold and window depth 5; (d) image reconstructed based on variable threshold and window depth 10.

(a) (b) (c) (d)

(e) (f) (g) (h)

Figure C7 A frame of the video. (a) is the first frame of the original video. (b), (c), and (d) are the reconstructed frame based on fixed threshold with I_{pmax} set to 3 pA, 15 pA and 45 pA, respectively. (e) is the frame of the original video corresponding to the reconstructed frame shown in other sub images. (f), (g), and (h) are the reconstructed video based on variable threshold with I_{pmax} set to 3 pA, 15 pA and 45 pA, respectively.

Table C3 MSE results of the frame shown in Figure C7

I_{pmax}(pA)	3	15	45
MSE with fixed threshold	73.4494	11.5455	58.6560
MSE with variable threshold	3.0279	4.4966	1.4732

$$MSE_{\mathrm{video}} = \frac{1}{f}\sum_{k=f_{\mathrm{s}}}^{f_{\mathrm{s}}+f} MSE\,(k) \tag{C4}$$

where parameter f is the number of frames used to compute MSE, parameter f_{s} is the first frame of the video. The MSE results of the reconstructed videos are shown in Figure C8 and Table C4.

In reconstructed videos with fixed threshold, the MSE is relatively small in medium illumination section. As shown in Figure C7(c), the frame constructed with maximum mapping photocurrent in the section shows great quality. In the low illumination section, the integration time is longer and the pixel pulse may not response to the change of photocurrent in real time. As maximum mapping photocurrent decreases to 3 pA, the MSE increases to 86.6751 and image lag appears. The edge of fingers is obviously blurred in Figure C7(b). In high illumination section, the integration time is much shorter and

Table C4 MSE results of the reconstructed videos

I_{pmax}(pA)	3	7	11	15
MSE with fixed threshold	86.6751	24.6989	14.9585	13.6346
MSE with variable threshold	5.0713	3.1686	3.5949	4.4886
I_{pmax}(pA)	19	23	27	31
MSE with fixed threshold	16.3677	19.9582	26.4786	31.5715
MSE with variable threshold	4.1810	3.7772	3.7065	4.3040
I_{pmax}(pA)	35	39	43	45
MSE with fixed threshold	42.0899	48.9721	59.3795	59.4343
MSE with variable threshold	4.0923	4.0896	4.6782	5.2646

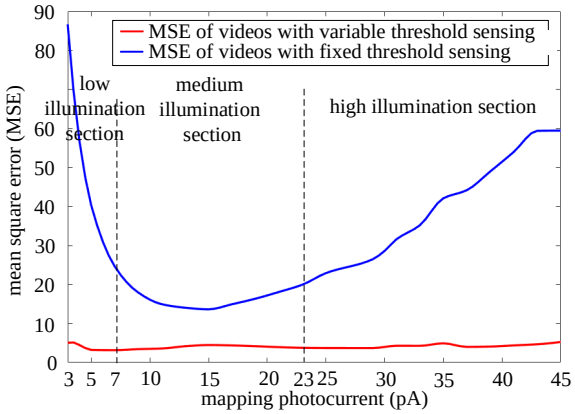

Figure C8 MSE results of videos with different maximum mapping photocurrent.

pixel pulse are able to response to the change of photocurrent in real time. In Figure C7(d), the image lag disappears. But obvious overexposure appears in the neck and face because some gray levels are lost. With maximum mapping photocurrent increases to 45 pA, the MSE increases to 59.4343. There is a tradeoff between the responding speed and the image quality in video reconstructed with fixed threshold.

In reconstructed videos with variable threshold and different maximum mapping photocurrent, the MSE results are lower than 5.2646 and the frames show high similarity to the original frame. Because the variable threshold increases from the fixed threshold V_{th0}, pixels' integration time is shorter than that of pixels working with fixed threshold under the same light conditions. As a result, the reconstructed video shows better performance when I_{pmax} is low. As shown in Figure C7(f), there is no image lag with I_{pmax} as low as 3 pA. When I_{pmax} is high, video reconstructed based on variable threshold shows better image quality and richer information as shown in Figure C7(h). It can be concluded that the proposed method is less sensitive to the change of light conditions and shows better performance than the traditional method with fixed threshold.